Environmental Science & Technology

Article

pubs.acs.org/est

Antifouling Action of Polyisoprene-Based Coatings by Inhibition of Photosynthesis in Microalgae

Rachid Jellali,[†] Jacco C. Kromkamp,[‡] Irène Campistron,[†] Albert Laguerre,[†] Sébastien Lefebvre,[§] Rupert G. Perkins,[∥] Jean-François Pilard,[†] and Jean-Luc Mouget*[,⊥]

[†]UMR CNRS N° 6283, Méthodologie et Synthèse des Polymères, Département Méthodologie et Synthèse, Institut des Molécules et des Matériaux du Mans, Université du Maine, Avenue Olivier Messiaen, 72085 Le Mans Cedex 9, France

[‡]Department of Marine Microbiology, Royal Netherlands Institute for Sea Research (NIOZ), P.O. Box 149, 4400 AC, Yerseke, The Netherlands

[§]Université de Lille1 Sciences et Technologies – CNRS, UMR 8187 LOG (Laboratoire d'Océanologie de Géosciences), Station Marine de Wimereux, 28 av. Foch, 62930 Wimereux, France

[∥]School of Earth and Ocean Sciences, Cardiff University, Cardiff, Wales CF10 3AT, United Kingdom

[⊥]EA 2160 (MMS, Mer, Molécules, Santé), Faculté des Sciences, Université du Maine, Avenue Olivier Messiaen, 72085 Le Mans Cedex 9, France

ABSTRACT: Previous studies have demonstrated that ionic and non-ionic natural rubber-based coatings inhibit adhesion and growth of marine bacteria, fungi, microalgae, and spores of macroalgae. Nevertheless, the mechanism of action of these coatings on the different micro-organisms is not known. In the current study, antifouling activity of a series of these rubber-based coatings (one ionic and two non-ionic) was studied with respect to impacts on marine microalgal photosynthesis using pulse-amplitude-modulation (PAM) fluorescence. When grown in contact with the three different coatings, an inhibition of photosynthetic rate (relative electron transport rate, rETR) was observed in all of the four species of pennate diatoms involved in microfouling, *Cocconeis scutellum*, *Amphora coffeaeformis*, *Cylindrotheca closterium*, and *Navicula jeffreyi*. The percentage of inhibition ranged from 44% to 100% of the controls, depending on the species and the coating. The ionic coating was the most efficient antifouling (AF) treatment, and *C. scutellum* and *A. coffeaeformis* are the most sensitive and tolerant diatoms tested, respectively. Photosynthetic inhibition was reversible, as almost complete recovery of rETR was observed 48 h post exposure, after detachment of cells from the coatings. Thus, the antifouling activity seemed mostly due to an effect of contact with materials. It is hypothesized that photosynthetic activity was suppressed by coatings due to interference in calcium availability to the microalgal cells; Ca^{2+} has been shown to be an essential micro/macro nutrient for photosynthesis, as well as being involved in cell adhesion and motility in pennate diatoms.

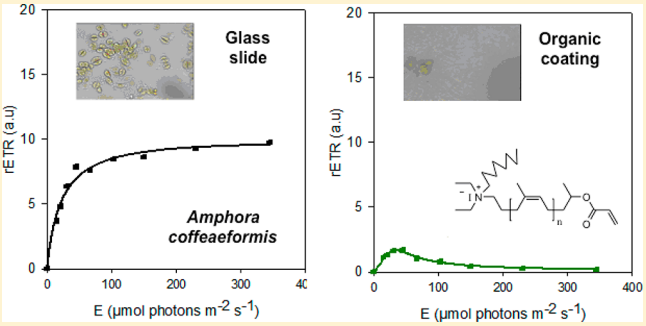

INTRODUCTION

Biofouling is the undesirable accumulation of micro- and macro-organisms on submerged surfaces. This phenomenon concerns a great variety of structures such as ships and marine platforms,[1−4] as well as offshore rigs, jetties, and aquaculture enterprises.[5−8] Biofouling is a major economic and technical problem. It is estimated that biofouling causes direct or indirect losses equivalent to 7% of the gross national product in countries having a marine industry.[9] Efficient antifouling (AF) protection would allow saving over 150 billion USD per year in 2020.[10] It is generally agreed that the prevention of marine fouling can be achieved by the use of coatings, which provide a controlled release of toxic molecules. During the last decades, tributyltin self-polishing copolymer paints (TBT-SPC paints) have been the most successful in combating biofouling on ships.[1] The widespread use of these paints, estimated to cover 70% of the total world fleet,[11] led to significant economic benefits. Unfortunately, as an environmental counterpart, these formulations seriously impacted upon marine ecosystems.[12−14] As a consequence, the use of TBT in small boats (less than 25 m in length) has been prohibited in many countries since the mid-1980s. An international convention held on 5 October 2001 banned the application of TBT-based antifouling (AF) paints by 1 January 2003 and imposed a complete prohibition of the presence of such paints on ship surface by 1 January 2008.

Received: January 12, 2013
Revised: May 6, 2013
Accepted: May 13, 2013

   dx.doi.org/10.1021/es400161t | Environ. Sci. Technol. XXXX, XXX, XXX−XXX

The paint industry has been urged to develop TBT-free products as antifoulant replacements, yielding the same economic benefits but causing less harmful impacts upon the environment. Some supposedly less toxic materials are already being used, such as low molecular weight products (organic biocides: Irgarol 1051, zinc pyrithione, Diuron, Sea-Nine 211, Zineb) incorporated in a matrix used for the hull coating.[3,15,16] The toxicity of these products has not been sufficiently well studied yet. However, several works have highlighted that these compounds are also harmful to the environment.[16,17] Nonstick fouling-release coatings based on fluoropolymer and silicon have also been developed.[16] A promising alternative to these is to covalently bind biocidal functions on a polymer chain to avoid the release of biocide products and maintain a permanent AF activity on the ship hulls. Hence, a number of biocidal agents, such as quaternary ammonium (QA) salts, phosphonium salts, sulfonium salts, chlorophenyl derivatives, and N-halamine, have been introduced into ordinary polymers. In antifouling paints, QA salts are essentially found in polymers including polyurethanes,[18,19] polysiloxane,[20−22] and polymethacrylates.[23−25]

Recent experiments were conducted by developing ionic (with QA) and non-ionic coatings from different polymers stemming from renewable resources (natural rubber) and studying their AF activity. For example, one previous study describes the synthesis of ionic and non-ionic coatings by photo-cross-linking of various oligoisoprenes.[26,27] These coatings present an important inhibition effect against the adhesion and growth of marine bacteria, fungi, microalgae, and spores of macroalgae, where the presence of QA groups in coatings increasing the AF activity.[28,29] AF and/or antibacterial activities of polyisoprene derivatives[30] or similar products (terpenes, composed of units of isoprene)[31−33] and ionic coatings based QA groups[18−25] are well known and have been reported in many studies. However, the possible mechanisms of AF action were not investigated. Concerning antibacterial effects of QA groups, it is known that ionic coatings with QA exert their biocidal activity by interaction with the cell wall of bacteria.[18,34−36] In particular, electrostatic interactions could be responsible for the effect of QA groups on membrane lipids.[37] In contrast, for eukaryotic organisms, more specifically for microalgae, macroalgae, and fungi, the mechanisms of action remains unknown. Thus, this study focused on the AF effect and the mechanism of action of ionic and non-ionic polyisoprene-based coatings against benthic microalgae by studying their photosynthetic activity using pulse-amplitude-modulation (PAM) fluorescence, using a single-cell fluorescence technique (microscopy imaging fluorimeter). Significant differences in the photosynthetic characteristics of microalgae, including those able to adhere to the coatings and species unable to adhere, were observed. Results are discussed with respect to the role of calcium ions both for adhesion, motility, and photosynthetic activity in different species of benthic diatoms involved in microfouling.

MATERIALS AND METHODS

Synthesis and Preparation of Coatings. Coatings investigated in this work can be divided into two main groups: ionic (R9) and non-ionic (R1 and R2) coatings. Chemical structures of the different compounds used for coating elaboration are shown in Figure 1. Acrylate cis-1,4-polyisoprene cationomer (acrylate PI cationomer), epoxidized hydroxytelechelic cis-1,4-polyisoprene (EHTPI), and diacrylate cis-1,4-polyisoprene (diacrylate PI) were synthesized from hydroxyltelechelic cis-1,4-polyisoprene according to a methodology previously described.[26−28] Coatings were prepared by radical or cationic photopolymerization under UV radiation. Table 1 represents the combinations of oligomers used for the different coatings. The synthesis method involved the photopolymerization reaction of the acrylate (radical process) or epoxid (cationic process) groups of the oligomers in the presence of photoinitiators: 2,2-dimethyl-2-hydroxyacetophenone (Darocur 1173, Aldrich, Figure 1) or hexafluoro-phosphate triarylsulfonium salt (Degacur KI85, Aldrich, Figure 1) for the radical and cationic polymerization, respectively. The mixtures (oligoisoprene and photoinitiator) were spread on a range of surfaces (glass, plexiglass (PMMA), and polytetrafluoroethylene (PTFE)) and then exposed to UV radiation for 10 min with a 350 W Oriel mercury vapor lamp (polychromatic lamp, maximum emission at 365 nm). The intensity of irradiation was 30 mW/cm^2 and 50 mW/cm^2 for radical (R2 and R9) and cationic (R1) polymerization, respectively (optimal conditions).[26,27] The thickness of resulting coatings was between 0.5 and 0.8 mm. After curing, synthesis residues and possible free oligomers were extracted with dichloromethane using a Soxhlet extractor over 24 h at 40 °C. Finally, samples were removed from the solvent and dried under reduced vacuum.

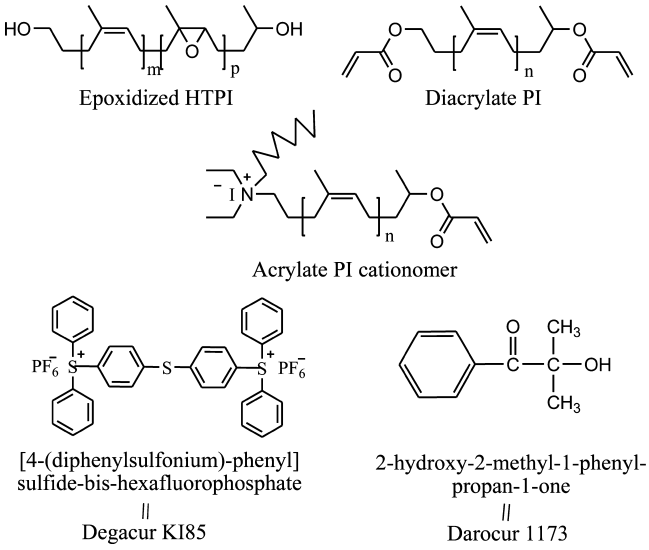

Figure 1. Chemical structures of the different oligoisoprenes and of the photoinitiators used for the experiments.

Table 1. Composition of the Different Coatings Tested

coating code	precursors	photoinitiator (2.5%, w/w)
R1	EHTPI 25%[a]	Degacur KI85
R2	diacrylate PI[b]	Darocur 1173
R9	diacrylate PI and acrylate PI cationomer [75/25 (w/w)]	Darocur 1173

[a]Epoxidation rate. EHTPI: epoxidized hydroxytelechelic cis-1,4-polyisoprene. [b]PI: polyisoprene.

Physico-Chemical Properties of Coatings. Stability of the coatings under water was determined by immersing material in fresh water and seawater. After four weeks, samples were removed from the water, weighed (m_s) and dried under reduced vacuum until a constant mass was obtained (m_f). The

dx.doi.org/10.1021/es400161t | Environ. Sci. Technol. XXXX, XXX, XXX−XXX

swelling percentage W_s (%) and weight loss (W_l) were then calculated using equations 1 and 2

$$W_s(\%) = \frac{m_s - m_0}{m_0} \times 100 \quad (1)$$

$$W_l(\%) = \frac{m_0 - m_f}{m_0} \times 100 \quad (2)$$

where m_s is the weight of the swollen film, m_f is the final weight (after drying) and m_0 is the weight of the original dry film.

Surface energies of the materials were evaluated using a GBX goniometer to measure the static contact angle (θi) with three liquids: water, diiodomethane, and formamide. According to the Owens–Wendt relationship (eq 3), the dispersive γ_S^d and polar γ_S^p components of the surface energies $\gamma_S = \gamma_S^p + \gamma_S^d$ of the coatings were determined

$$\frac{(1 + \cos\theta_i)\gamma_i}{2\sqrt{\gamma_i^d}} = \sqrt{\gamma_s^p} \times \sqrt{\frac{\gamma_i^p}{\gamma_i^d}} + \sqrt{\gamma_s^d} \quad (3)$$

where γ_i, γ_i^p, and γ_i^d are the solvent superficial tension parameters. Surface polarities (P) of the coatings were calculated using

$$P = (\gamma_s^p/\gamma_s) \times 100 \quad (4)$$

Atomic force microscopy (AFM) images were recorded in the tapping mode with a Nanoscope II from Digital Instruments, with a 120 μm piezoelectric scanner. The polymer mixtures were cast on silica substrates and irradiated for 10 min under UV irradiation. The obtained films were observed by AFM in height (roughness measurement) and phase modes.

Biological Material and Culturing. The marine diatoms tested are common species observed in microfouling biofilms.[38,39] *Cylindrotheca closterium* (NCC36) and *Cocconeis scutellum* (NCC209) were obtained from the Nantes Culture Collection (NCC) at Nantes University. *Navicula jeffreyi* and *Amphora coffeaeformis* were obtained from Portsmouth University, U.K., and Montana State University, U.S.A., respectively. Microalgae were cultivated in an artificial seawater medium (ASW).[40] Stock cultures were grown in 250 mL Erlenmeyer flasks containing 150 mL of ASW and incubated in a temperature-controlled culture chamber (15 ± 1 °C), under a 14 h:10 h light:dark cycle and a constant irradiance (100 μmol photons m^{-2} s^{-1}) provided by daylight fluorescent tubes. Algal cultures were maintained in exponential growth by regular dilution with fresh medium (semi-continuous culture mode), ensuring similar biomass levels and hence physiological status for each series of experiments. Agitation was provided by hand shaking once a day.

For each series of experiments, the impact of coatings on the photosynthetic activity was estimated using in vivo chlorophyll *a* (Chl *a*) fluorescence measured on single cells, either adhered to a surface or in suspension. For adhered cells, discs of the different coatings were placed in Petri dishes, with a glass slide being used as control. The complete setup was sterilized under UV irradiation for 30 min. The different microalgal suspensions were diluted with fresh ASW medium to a final volume of 10 mL and a cell final concentration of 75 000 cells mL^{-1} under aseptic conditions and poured on the coatings. The Petri dishes were then incubated for 5 days in the culture room (15 ± 1 °C, 100 μmol photons m^{-2} s^{-1}, 14 h:10 h light:dark cycle), a period that allowed the controls to reach an exponential growth phase. Three series of experiments were completed (1) on cells adhered to the coatings, (2) on cells in suspension, and (3) on cells detached from the coatings after a 48 h recovery period. The AF effect of the coatings was first observed on cells adhered to the different surfaces. After 5 days, the discs were rinsed three times with seawater and placed between a microscope slide and a coverslip for photosynthetic activity estimation. For the measurement of photosynthesis on cells in suspension, samples were pipetted onto a microscope slide and covered with a cover glass. For the recovery experiments, cells that adhered to the coatings were gently detached and resuspended in Petri dishes containing fresh ASW medium for a 48 h recovery period.

Measure of Photosynthesis. Three series of experiments were conducted using cells collected in suspension or cells adhered on coatings: (1) assessment of AF activity of the three different coatings (R1, R2, R9) against the four diatoms species (*C. closterium, C. scutellum, N. jeffreyi*, and *A. coffeaeformis*), (2) assessment of biocide release using the R9 coating and two species, *C. closterium* and *A. coffeaeformis*, and (3) measurement of the photosynthetic recovery of algal cells that had been significantly but differently impacted by AF treatment (*C. closterium* and *A. coffeaeformis*) after their detachment from the AF treated surface discs (R9 coating).

In vivo Chl *a* fluorescence of individual cells was measured using a microscopy-PAM fluorimeter (Heinz Walz, Effeltrich, Germany) according to methodology described by Dijkman and Kromkamp.[41] The microscopy-PAM was attached to an epifluorescence microscope (Axiostar plus, Zeiss) and used blue LEDs at 470 nm for measuring modulated light, saturating flashes, and actinic irradiance. Fluorescence measurements were performed at a magnification of 40x on single cells either pippeted from the suspension (non-adherent cells) and deposited on microscope slides or adhered directly on a surface (adherent cells on coatings, or a glass slide for control) and laid on a microscope slide. All preparations were covered with a coverslip. Either from the suspension or present on the coating, microalgal cells were centered in the light field of the microscope to detect fluorescence emission and measure photosynthetic activity. A custom-built slide holder connected to a cryostat was used to maintain a sample at the growth temperature during fluorescence measurements. Photosynthetic activity was estimated as relative electron transport rate (rETR), and photosynthesis light response (rETR/E) curves were obtained using the rapid light curve (RLC) technique.[40]

RLCs were performed using 20 s exposure duration at each actinic light level after an initial quasi-dark measurement (ca. 15 min at light level <1.5 μmol photon m^{-2} s^{-1}) to obtain proxy values of F_0 and F_m, the minimum and maximum fluorescence yields in a dark-acclimated sample, respectively. These parameters were used to calculate the variable fluorescence $(F_m - F_0) = F_v$ and the maximum quantum yield of PSII in a dark-acclimated sample F_v/F_m. A complete RLC consisted in nine incremental irradiances (15, 21, 31, 45, 67, 103, 150, 230, and 345 μmol photons m^{-2} s^{-1}) and was constructed by calculating rETR according to eq 5

$$\text{rETR} = E \times (F_m' - F_t)/F_m' \times 0.5 \quad (5)$$

where F_m' is the maximum fluorescence yield in a light-acclimated sample, F_t the instantaneous fluorescence yield, and $(F_m' - F_t)/F_m'$ represents the effective quantum yield of PSII. The actinic irradiance E is in μmol photons m^{-2} s^{-1}, and 0.5 is a multiplication factor based on the assumption that 50% of the absorbed quanta are distributed to PSII.[42]

dx.doi.org/10.1021/es400161t | Environ. Sci. Technol. XXXX, XXX, XXX–XXX

Statistics. The light (E) response of rETR or rETR/E curves were constructed using the model of Eilers and Peeters[43] using three replicates of RLCs simultaneously in the same model, using the eq 6

$$\mathrm{rETR} = \frac{E}{aE^2 + bE + c} \quad (6)$$

The variables (a), (b), and (c) are adjustment parameters for the model. Then, photosynthetic parameters α (photosynthetic rate in the light-limited region), E_k (minimum saturating irradiance), and rETR_{max} (relative maximum electron transport rate) were determined according to the following equations

$$\alpha = \frac{1}{c}$$

$$\mathrm{rETR}_{max} = \frac{1}{(b + 2\sqrt{ac})}$$

$$E_k = \frac{c}{(b + 2\sqrt{ac})}$$

Curve fitting was achieved using the downhill simplex method of the Nelder-Mead model,[44] and standard deviation of parameters was estimated by an asymptotic method. All fittings were tested by analysis of variance ($P < 0.001$), residues being tested for normality and homogeneity of variance and parameter significance by Student's t test ($P < 0.05$). Comparisons of RLCs were performed using the method of Ratkowski[45] for non-linear models. All the curve fitting processes and associated statistics were coded under MATLAB R2008b.

RESULTS AND DISCUSSION

In a previous study, new possibly environment-friendly antifouling (AF) coatings using oligoisoprenes bearing a variable number of ammonium groups were described, and their surface properties evaluated.[26−29] The AF capacity of these coatings was tested against several strains of marine bacteria, microalgae, fungi, and spores of one macroalga.[28,29] In this study, the AF activity of three isoprene-based coatings were more specifically studied against four marine diatoms by focusing on the inhibition of the photosynthetic activity.

Characteristics and Specificities of Different Coatings Tested. Three different polymer materials were elaborated from the previously described cis-1,4-polyisoprene oligomers (Figure 1),[26−28] one ionic coating (R9), and two non-ionic coatings based on epoxidized HTPI (R1) or on diacrylate PI (R2). Oligomers were mixed (various formulations are reported in Table 1) with photoinitiators, spread on microscope slides, and exposed to the UV lamp. The photopolymerization reaction was run as previously described.[26,27] Surface properties of three coatings used in this work are mentioned in Table 2. The stability of the polymers in an aqueous environment was investigated by immersing samples in water and seawater for four weeks. For materials synthesized by radical process (R2 and R9), neither swelling in water nor weight loss were observed. A light swelling (5%) was observed for the material elaborated by cationic photo-cross-linking (R1). This result shows a strong stability in water as well as a strong hydrophobic character in spite of the presence of hydrophilic ammonium groups. This property suggests that these coatings are suited for applications in which they would be hydrated. Ionic coating (R9) and non-ionic coating elaborated using epoxidized PI (R1, cationic photopolymerization) are more polar than material obtained using diacrylate PI (R2, radical photopolymerization) due to the ammonium functions, hydroxy functions, and ether bridges, respectively. However, for all the materials, surface polarities were lower than 50%, confirming their hydrophobic character, which was already observed in the swelling tests.

Table 2. Surface Properties of Coatings

	weight loss	swelling rate (%)	polarity (%)	roughness (Å)
R1	0	5	20	47
R2	0	0	7	18
R9	0	0	10	nd[a]

[a]nd: not determined.

AFM was used to examine roughness and surface morphology. The roughness of the materials synthesized by cationic process (47 Å for R1) was higher than those of the materials elaborated by radical process (18 Å for R2) due to higher cross-linking density: organization of polymer networks decreased as cross-linking density increased. Because of technical constraints, roughness for R9 is not available, but it should be in the range of values observed for other coatings synthesized by radical process (<20 Å). The phase images show no specific surface morphology.

Inhibition of Photosynthetic Activity in Microalgae in Contact with Coatings. For this first series of experiments, the three coatings (R1, R2, R9) were immersed in the different microalgal suspensions for 5 days. The coatings were rinsed to eliminate the non-adherent cells, and the photosynthetic activity of attached microalgae was determined using single-cell fluorimetry (microscopy-PAM). The rETR/E curves and the different photosynthetic parameters are shown in Figure 2 and Table 3, respectively.

The relative maximum electron transport rate (rETR_{max}) and the maximum quantum yield of charge separation in PSII (F_v/F_m) of adherent microalgae were significantly reduced ($P < 0.001$) when algae were in contact with the coatings. On average, for all coatings and species tested, rETR_{max} decreased to 14.8 ± 5.3% of the controls (mean ± SEM, $n = 12$). The photosynthetic rate in the light-limited region (α) and the minimum saturating irradiance (E_k) were also considerably reduced (15.7 ± 5.5% and 75.6 ± 35.0% of the controls, respectively), indicating that all coatings had an important inhibitor effect on the photosynthetic activity. However, the magnitude of photosynthetic inhibition varied between the strains of microalgae and the nature of the coating.

The ionic coating (R9) almost completely inhibited the photosynthetic activity for all diatom species tested (2.9% of the controls), the most resistant being *A. coffeaeformis*, with a low rETR_{max} (14.6% of the control). For the non-ionic coatings, the photosynthetic activity was impacted to a lower extent, highly reduced in *A. coffeaeformis* and *N. jeffreyi* and completely inhibited in *C. closterium* and *C. scutellum* (R2) and highly reduced but not completely inhibited for the four species (R1). The decrease in ETR_{max} was higher in R2 (11.2%) than in R1 (23.7%). This result confirms the antialgal effects previously evidenced by comparing growth of algae in presence or in absence of coatings and the increase in the antifouling action by the addition of quaternary ammonium groups in the coatings, as observed in R9. If we consider the overall effect of the three different coatings, the decrease in rETR_{max} was lower (26.5%) for *A. coffeaeformis* than in the three other species (10.9% on

dx.doi.org/10.1021/es400161t | Environ. Sci. Technol. XXXX, XXX, XXX−XXX

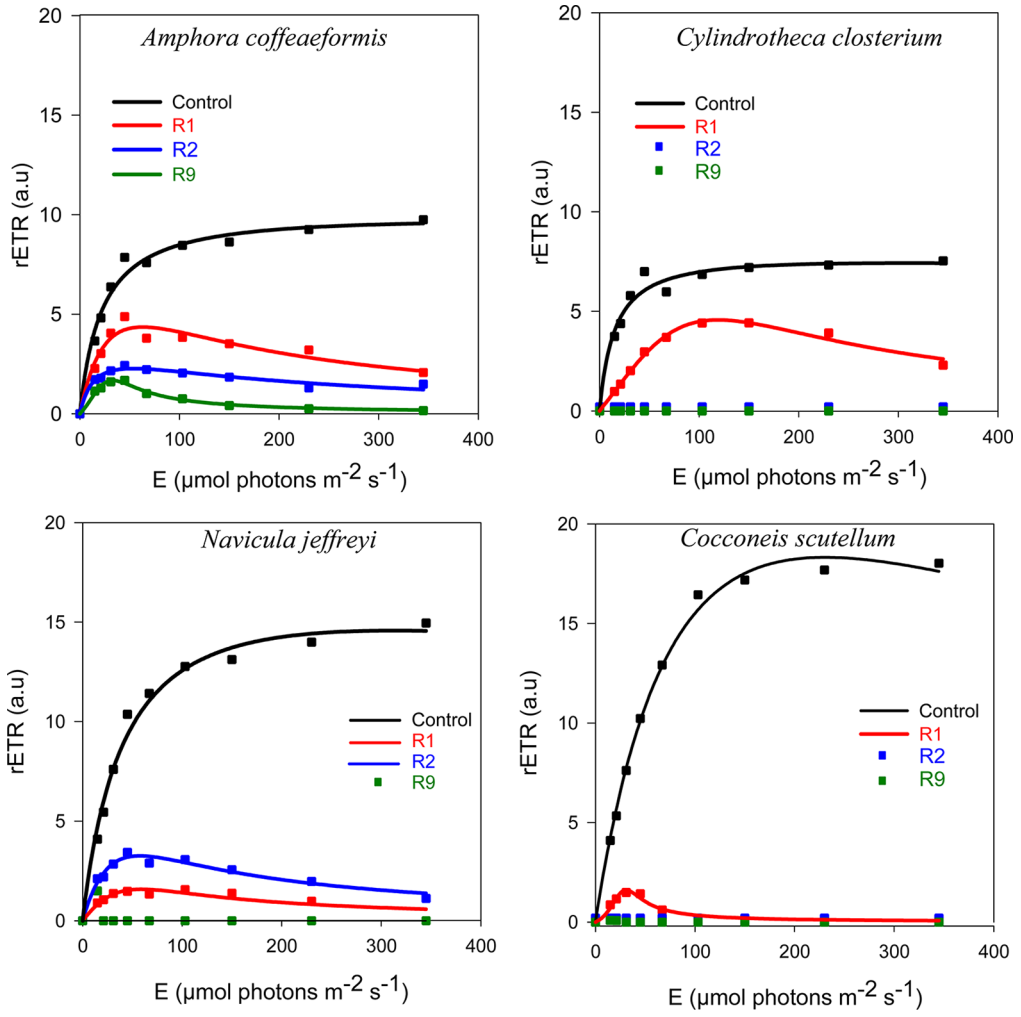

Figure 2. Photosynthesis versus irradiance (rETR/E) curves for *Amphora coffeaeformis*, *Cylindrotheca closterium*, *Navicula jeffreyi*, and *Cocconeis scutellum* adherent in the various coatings and surface (R1, R2, R9, and control = glass). Each observation is a mean of three different experiments, solid line representing model results (see Materials and Methods for details on statistic analyses).

Table 3. Photosynthetic Parameters as Determined by Fitting Using Eilers and Peeters Model on RLCs[a]

		A. coffeaeformis	*C. closterium*	*N. jeffreyi*	*C. scutellum*
control	F_v/F_m	0.486 ± 0.007	0.499 ± 0.004	0.546 ± 0.011	0.547 ± 0.018
	$rETR_{max}$	10.18 ± 0.39	7.87 ± 0.23	14.57 ± 3.05	18.31 ± 2.66
	α	0.48 ± 0.06	0.56 ± 0.07	0.42 ± 0.02	0.32 ± 0.02
	E_k	21.16 ± 2.80	13.93 ± 1.78	34.53 ± 7.37	56.45 ± 8.81
R1	F_v/F_m	**0.303 ± 0.009**	**0.130 ± 0.023**	**0.120 ± 0.018**	**0.116 ± 0.013**
	$rETR_{max}$	**4.35 ± 0.47**	**4.41 ± 0.41**	**1.62 ± 0.88**	**1.60 ± 0.06**
	α	**0.24 ± 0.02**	**0.07 ± 0.00**	**0.05 ± 0.02**	**0.02 ± 0.00**
	E_k	17.85 ± 2.25	*60.58 ± 6.80*	29.96 ± 19.94	*71.02 ± 3.08*
R2	F_v/F_m	**0.229 ± 0.020**	**0.000 ± 0.000**	**0.281 ± 0.036**	**0.000 ± 0.000**
	$rETR_{max}$	**2.27 ± 0.78**	nd	**3.25 ± 0.66**	nd
	α	**0.21 ± 0.05**	nd	**0.17 ± 0.02**	nd
	E_k	**10.72 ± 4.50**	nd	**18.81 ± 4.27**	nd
R9	F_v/F_m	**0.151 ± 0.023**	**0.000 ± 0.000**	**0.200 ± 0.162**	**0.011 ± 0.006**
	$rETR_{max}$	**1.49 ± 0.43**	nd	nd	nd
	α	**0.10 ± 0.02**	nd	nd	nd
	E_k	14.83 ± 5.39	nd	nd	nd

[a] (n = 27/species and treatment. For treatments R1, R2, R9, values in bold (decrease) and italic (increase) are significantly different from the control (see Materials and Methods for details): maximum relative electron transport rate ($rETR_{max}$), maximum quantum yield of charge separation in PSII (F_v/F_m), photosynthetic rate in light-limited region (α), and light saturating irradiance (E_k) of *A. coffeaeformis*, *C. closterium*, *N. jeffreyi*, and *C. scutellum* adherent in the various coatings and surface (R1, R2, R9, and glass = control). nd = not determined.

dx.doi.org/10.1021/es400161t | *Environ. Sci. Technol.* XXXX, XXX, XXX−XXX

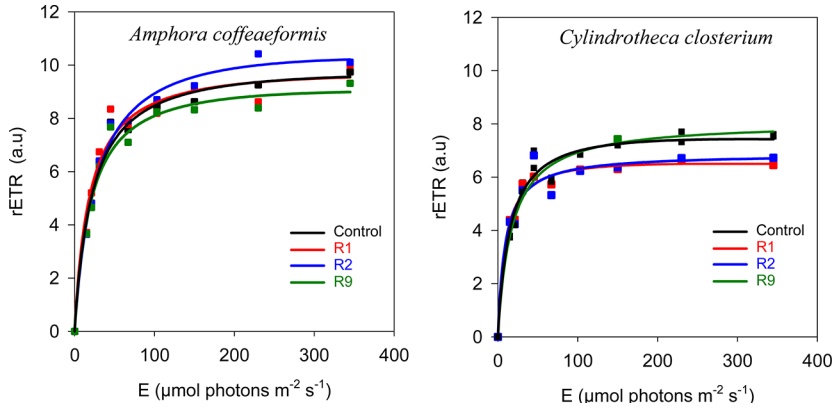

Figure 3. Photosynthesis versus irradiance (rETR/E) curves for *Amphora coffeaeformis* and *Cylindrotheca closterium* cultivated in presence in various coatings and surface (R1, R2, R,9 and glass = control). Each observation is a mean of three different experiments (see Materials and Methods for details on statistic analyses).

Table 4. Photosynthetic Parameters[a]

		control	R1	R2	R9
A. coffeaeformis	F_v/F_m	0.486 ± 0.007	0.495 ± 0.014	0.487 ± 0.009	0.489 ± 0.007
	$rETR_{max}$	10.18 ± 0.39	10.12 ± 0.36	11.03 ± 0.51	9.61 ± 0.50
	α	0.48 ± 0.06	*0.55 ± 0.07*	**0.44 ± 0.06**	0.49 ± 0.09
	E_k	21.16 ± 2.80	18.55 ± 2.44	24.94 ± 3.70	19.60 ± 3.68
C. closterium	F_v/F_m	0.499 ± 0.004	*0.585 ± 0.006*	*0.576 ± 0.015*	0.505 ± 0.004
	$rETR_{max}$	7.87 ± 0.23	**6.73 ± 0.13**	**6.88 ± 0.17**	8.10 ± 0.15
	α	0.56 ± 0.07	*0.82 ± 0.09*	*0.75 ± 0.10*	0.47 ± 0.03
	E_k	13.93 ± 1.78	**8.17 ± 0.90**	**9.22 ± 1.25**	17.16 ± 1.22

[a]Maximum electron transport rate ($rETR_{max}$), maximum quantum yield of charge separation in PSII (F_v/F_m), photosynthetic rate in light-limited region (α), and minimum saturating irradiance (E_k) of *A. coffeaeformis* and *C. closterium* cultivated in presence in various coatings and surface (R1, R2, R9, and glass = control). For treatments R1, R2, R9, values in bold (decrease) and italic (increase) are significantly different from the control (see Materials and Methods for details).

the average). This could be due to the fact that *A. coffeaeformis* was less sensitive to the chemical nature of the coating and its possible mode of action, in the same way this species has been demonstrated to be tolerant to a self-polishing organotin AF paint[46] or because it produced more extracellular polymeric substances (EPS), which could act as a protective barrier.[47]

Inhibition of Photosynthetic Activity Is Not Due to Release of Biocide by Coatings. In a previous work, it was observed that growth kinetics of *A. coffeaeformis* cultured in batch mode in the presence or absence of the R9 coating were not different.[29] Thus, the purpose of this series of experiments was to test the hypothesis that the release by the coatings of biocide agents in the culture medium could be responsible for the decrease in photosynthetic activity as opposed to direct AF activity of the coated surface. Two species for which significant differences in photosynthetic activity were observed between coatings and controls, *A. coffeaeformis* and *C. closterium*, were grown in Petri dishes containing 10 mL of ASW (total volume) and one of the different coatings to be tested (R1, R2 and R9) and compared to control cultures without coatings. After 5 days, when microalgae were in the exponential phase of growth, the photosynthetic activities of cells in suspension in the medium (not in contact with the coating) were estimated using the microscopy-PAM. The rETR/E curves and the different photosynthetic parameters are shown in Figure 3 and Table 4, respectively. For both species, no significant differences ($P > 0.05$) for all photosynthetic parameters were observed for the coating treatments when compared to the control (no coating) for all coatings and material discs used. The photosynthetic parameters of algae cultivated in the presence of R1, R2, and R9 coatings were almost identical to the photosynthetic parameters of the algae cultivated without coatings (control). These results indicate an absence of biocidal moieties released during the immersion of coatings in the culture medium, thus confirming that the coatings were active by contact only, as previously observed by an inhibition of algal growth.[29] These results demonstrate the absence of inhibition of photosynthesis in microalgae and, hence, the absence of an observable toxic AF activity by the three AF materials tested on microalgal cells maintained in suspension and therefore not in direct contact with the coatings.

Reversibility of Photosynthesis Inhibition Effect. For this series of experiments, microalgae adherent to the coatings and having demonstrated a reduced photosynthetic activity were gently detached by vortex agitation in fresh ASW medium. Then, the algae were resuspended in Petri dishes containing fresh ASW medium (total volume = 10 mL) and placed back in the culture room for a 48 h recovery period under the same light conditions (14 h:10 h light:dark cycle and constant 100 μmol photons m^{-2} s^{-1} irradiance). The experiments were run using the two species previously studied, *A. coffeaeformis* and *C. closterium*, with cells adherent to the most effective coating only (ionic coating R9). Furthermore *A. coffeaeformis* and *C. closterium* responded to the R9 coating contrastingly, the former being less inhibited than the latter. After the 48 h recovery, the fluorescence emission was measured, and the photosynthetic parameters were determined as previously described. The results presented in Figure 4 and Table 5

dx.doi.org/10.1021/es400161t | Environ. Sci. Technol. XXXX, XXX, XXX−XXX

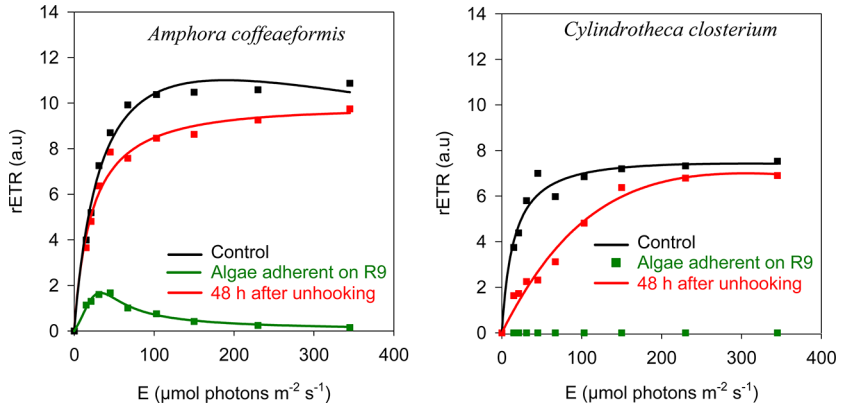

Figure 4. Photosynthesis versus irradiance (rETR/E) curves for *Amphora coffeaeformis* and *Cylindrotheca closterium* before and after unhooking of R9 coating. Each observation is a mean of three different experiments (see Materials and Methods for details on statistic analyses). For each species, significant differences between treatments were observed ($P < 0.001$).

Table 5. Photosynthetic Parameters[a]

	A. coffeaeformis				*C. closterium*			
	F_v/F_m	$rETR_{max}$	α	E_k	F_v/F_m	$rETR_{max}$	α	E_k
control	0.486 ± 0.007	10.18 ± 0.39	0.48 ± 0.06	21.16 ± 2.80	0.499 ± 0.004	7.87 ± 0.23	0.56 ± 0.07	13.93 ± 1.78
before detachment	**0.151 ± 0.023**	**1.49 ± 0.43**	**0.10 ± 0.02**	14.83 ± 5.39	**0.000 ± 0.000**	nd	n.d	nd
after detachment	*0.532 ± 0.005*	11.00 ± 1.20	0.43 ± 0.02	25.79 ± 3.00	**0,217 ± 0.009**	*9.61 ± 0.56*	**0.09 ± 0.01**	*106.40 ± 10.97*

[a]Maximum electron transport rate ($rETR_{max}$), maximum quantum yield of charge separation in PSII (F_v/F_m), photosynthetic rate in light-limited region (α), and minimum saturating irradiance (E_k) of *A. coffeaeformis* and *C. closterium* before and after detachment from R9 coating. Values in bold (decrease) and italic (increase) are significantly different from the control (see Materials and Methods for details). nd: not determined.

show a clear recovery of photosynthetic activity after detachment of the cells in both species. There were significant differences between species; the recovery was greatest for *A. coffeaeformis*, where the photosynthetic parameters had recovered to be almost identical to those of the controls. However, in *C. closterium*, the photosynthetic rate in the light-limited region remained significantly lower ($P < 0.01$) than those of the control. This difference could again reflect the specific high tolerance to the inhibition effect of AF coatings in *A. coffeaeformis*. Regarding *C. closterium*, it can be hypothesized that after detachment this species needed more time to recover and display a photosynthetic activity comparable to the control. Unfortunately, for time constraints, it was impossible to extend the recovery period for more than 48 h. However the reason for this specific difference in the length of the recovery period deserves further work, in particular regarding other microalgae involved in the microfouling process, but this was beyond the objective of this study.

This study has demonstrated that the AF compounds tested were all contact toxins and did not inhibit cells in suspension, indicating a less potentially harmful impact at the ecosystem level. Additionally the study has demonstrated mechanistic action of the AF compounds through photosynthetic inhibition. However, a major finding of this study is the recovery of photosynthetic activity observed for *A. coffeaeformis* and *C. closterium,* which demonstrates the reversibility of the photosynthetic inhibition effect of the ionic coating (R9) tested. The R9 coating did not act as a biocide (irreversible damage) but did by way of an algistatic effect (reversible inhibition). This reversible effect could be the consequence of the low concentration in QA groups; depending on the concentration, quaternary ammonium salts may have a reversible, inhibition, or stimulatory activity on photosynthetic membranes.[48] Nevertheless, another factor could be responsible for this observed inhibition, by contact and reversible, as cells displayed recovery as soon as they were no longer adherent to the coating. It has long been known that the pools of calcium ions in cells and in the culture medium are involved both in adhesion and motility of benthic diatoms.[49−52] One potential mechanism for activity is through reduction of calcium ion availability, which could have multiple consequences. Indeed Ca^{2+} is an almost universal intracellular messenger in signal transduction in eukaryotic cells, as it is involved in the regulation of many developmental and physiological processes,[53] in particular by way of ion channels in the plasma membrane and generation of action potential.[54] Ca^{2+} is also an important factor for PSII fluorescence emission at room temperature, possibly by interacting with the electron transport rate or at the water splitting complex.[55,56] In particular, Ca^{2+} plays both structural and functional roles for water oxidation, acting as a Lewis acid and as a binding site to oxidize H_2O molecules to O_2.[57] Competition and charge interactions between the coatings and QA groups and divalent cations, especially Ca^{2+} bound on the membranes,[58] could change the availability of Ca^{2+}, thus decreasing both adhesion and electron transport rate and leading to the observed decrease in adhesion of microalgae and of their photosynthesis once they are in contact with the coatings. To expand our knowledge regarding the mechanisms of action of AF coatings, more experiments are needed to confirm this hypothesis, but it was beyond the scope of the present work.

In conclusion, one ionic and two non-ionic coatings were prepared and tested to study the potential photosynthesis inhibiting activity in four microalgal diatom strains. Photosynthetic measurements were obtained using single-cell in vivo Chl *a* fluorescence. A marked but reversible inhibition of the photosynthetic activity, as measured by relative electron transport rate (light curve parameters), was observed in all

dx.doi.org/10.1021/es400161t | *Environ. Sci. Technol.* XXXX, XXX, XXX−XXX

coatings and algae tested. All coatings demonstrated the absence of release of any biocidal molecules into the aqueous medium; the inhibition effect was only observed when microalgae were in contact with the coated surfaces. The presence of quaternary ammonium groups in the ionic coating (R9) possibly increased the inhibition effect. Although as yet unexplained, the mechanism of photosynthesis inhibition by the coatings has been demonstrated to be reversible, illustrating the potential of these new materials to develop more environment-friendly antifouling coatings.

AUTHOR INFORMATION

Corresponding Author

*Telephone: 33-2-43-83-32-42. Fax: 33-2-43-83-37-95. E-mail: Jean-Luc.Mouget@univ-lemans.fr.

Notes

The authors declare no competing financial interest.

ACKNOWLEDGMENTS

We thank C. Hellio for valuable discussions. One of us (J.-L.M.) gratefully acknowledges receiving financial help from Université du Maine.

REFERENCES

(1) Yebra, D. M.; Kiil, S.; Dam-Johansen, K. Antifouling technology: Past, present and future steps towards efficient and environmentally friendly antifouling coatings. *Prog. Org. Coat.* **2004**, *50*, 75−104.

(2) Beech, I. B.; Sunner, J. Biocorrosion: Towards understanding interactions between biofilms and metals. *Curr. Opin. Biotechnol.* **2004**, *15*, 181−186.

(3) Schultz, M. P.; Bendick, J. A.; Holm, E. R.; Hertel, W. M. Economic impact of biofouling on a naval surface ship. *Biofouling* **2011**, *27*, 87−98.

(4) Townsin, R. L. The ship hull fouling penalty. *Biofouling* **2003**, *19*, 9−15.

(5) Braithwaite, R. A.; McEvoy, L. A. Marine biofouling on fish farms and its remediation. *Adv. Mar. Biol.* **2005**, *47*, 215−252.

(6) Phillippi, A. L.; O'Connor, N. J.; Lewis, A. F.; Kim, Y. K. Surface flocking as a possible anti-biofoulant. *Aquaculture* **2001**, *195*, 225−238.

(7) Ross, K. A.; Thorpe, J. P.; Brand, A. R. Biological control of fouling in suspended scallop cultivation. *Aquaculture* **2004**, *229*, 99−116.

(8) Rao, T. S.; Aruna, J. K.; Chandramohan, P.; Panigrahi, B. S.; Narasimhan, S. V. Biofouling and microbial corrosion problem in the thermo-fluid heat exchanger and cooling water system of a nuclear test reactor. *Biofouling* **2009**, *25*, 581−590.

(9) Ananda Kumar, S.; Sasikumar, A. Studies on novel silicone/phosphorus/sulphur containing nano-hybrid epoxy anticorrosive and antifouling coatings. *Prog. Org. Coat.* **2010**, *68*, 189−200.

(10) Hellio, C.; Yebra, D. M. Introduction. In *Advances in Marine Antifouling Coatings and Technologies,*; Hellio, C, Yebra, D. M., Ed.; Woodhead Publishing: Cambridge, U.K., 2009; pp 1−16.

(11) Gerigk, U.; Schneider, U.; Stewen, U. The present status of TBT copolymer antifouling paints versus TBT-free technology. *Prepr. Ext. Abstr. - ACS Natl. Meet., Am. Chem. Soc., Div. Environ. Chem.* **1998**, *38*, 91−94.

(12) Alzieu, C. Tributyltin: Case study of a chronic contaminant in the coastal environment. *Ocean Coastal Manage.* **1998**, *40*, 23−36.

(13) McPherson, C. A.; Chapman, P. M. Copper effects on potential sediment test organisms: the importance of appropriate sensitivity. *Mar. Pollut. Bull.* **2000**, *40*, 656−665.

(14) Eklund, B. T.; Kautsky, L. Review on toxicity testing with marine macroalgae and the need for method standardization − exemplified with copper and phenol. *Mar. Pollut. Bull.* **2003**, *46*, 171−181.

(15) Lejars, M.; Margaillan, A.; Bressy, C. Fouling release coatings: A nontoxic alternative to biocidal antifouling coatings. *Chem. Rev.* **2012**, *112*, 4347−4390.

(16) Thomas, K. V.; Brooks, S. The environmental fate and effects of antifouling paint biocides. *Biofouling* **2010**, *26*, 73−88.

(17) Dafforn, K. A.; Lewis, J. A.; Johnston, E. L. Antifouling strategies: History and regulation, ecological impacts and mitigation. *Mar. Pollut. Bull.* **2011**, *62*, 453−465.

(18) Jason, A. G.; Stuart, L. C. Synthesis and characterization of non-leaching biocidal polyurethanes. *Biomaterials* **2001**, *22*, 2239−2246.

(19) Nurdin, N.; Helary, G.; Sauvet, G. Biocidal polymers active by contact. II. Biological evaluation of polyurethane coatings with pendant quaternary ammonium salts. *J. Appl. Polym. Sci.* **1993**, *50*, 663−670.

(20) Gottenbos, B.; Van Der Mei, H. C.; Klatter, F.; Nieuwenhuis, P.; Busscher, H. J. *In vitro* and *in vivo* antimicrobial activity of covalently coupled quaternary ammonium silane coatings on silicone rubber. *Biomaterials* **2002**, *23*, 1417−1423.

(21) Clarkson, N.; Evans, L. V. Further studies investigating a potential non-leaching biocide using the marine fouling diatom *Amphora coffeaeformis*. *Biofouling* **1995**, *9*, 17−30.

(22) Majumdar, P.; Lee, E.; Patel, N.; Ward, K.; Stafslien, S. J.; Daniels, J.; Chisholm, B. J.; Boudjouk, P.; Callow, M. E.; Callow, J. A.; Thompson, S. E. M. Combinatorial materials research applied to the development of new surface coatings IX: An investigation of novel antifouling/fouling-release coatings containing quaternary ammonium salt groups. *Biofouling* **2008**, *24*, 185−200.

(23) Ravikumar, T.; Murata, H.; Koepsel, R. R.; Russell, A. J. Surface-active antifungal polyquaternary amine. *Biomacromolecules* **2006**, *7*, 2762−2769.

(24) Kenawy, E. R.; Worley, S. D.; Broughton, R. The chemistry and applications of antimicrobial polymers: A state-of-the-art review. *Biomacromolecules* **2007**, *8*, 1359−1384.

(25) Kenawy, E. R.; Abdel-Hay, F. I.; El-Magd, A. A.; Mahmoud, Y. Biologically active polymers: VII. Synthesis and antimicrobial activity of some crosslinked copolymers with quaternary ammonium and phosphonium groups. *React. Funct. Polym.* **2006**, *66*, 419−429.

(26) Jellali, R.; Campistron, I.; Laguerre, A.; Pasetto, P.; Lecamp, L.; Bunel, C.; Mouget, J. L.; Pilard, J. F. Synthesis of new photocurable oligoisoprenes and kinetic studies of their radical photopolymerization. *J. Appl. Polym. Sci.* **2013**, *127*, 1359−1368.

(27) Jellali, R.; Campistron, I.; Laguerre, A.; Lecamp, L.; Pasetto, P.; Bunel, C.; Mouget, J. L.; Pilard, J. F. Synthesis and crosslinking kinetic study of epoxidized and acrylated/epoxidized oligoisoprenes: Comparison between cationic and radical photopolymerization. *J. Appl. Polym. Sci.* **2013**, *128*, 2489−2497.

(28) Bunel, C.; Campistron, I.; Hellio, C.; Jellali, R.; Laguerre, A.; Mouget, J. L.; Pilard, J. F. Patent WO 2010043800, 2010.

(29) Jellali, R.; Campistron, I.; Pasetto, P.; Laguerre, A.; Gohier, F.; Hellio, C.; Pilard, J. F.; Mouget, J. L. Antifouling activity of polyisoprene-based coatings made from new photocurable oligoisoprenes. *Prog. Org. Coat.* **2013**, DOI: 10.1016/j.porgcoat.2013.03.028.

(30) Kébir, N.; Campistron, I.; Laguerre, A.; Pilard, J. F.; Bunel, C.; Jouenne, T. Use of telechelic cis-1,4-polyisoprene cationomers in the synthesis of antibacterial ionic polyurethanes and copolyurethanes bearing ammonium groups. *Biomaterials* **2007**, *28*, 4200−4208.

(31) Maréchal, J. P.; Culioli, G.; Hellio, C.; Thomas-Guyon, H.; Callow, M. E.; Clare, A. S.; Ortalo-Magne, A. Seasonal variation in antifouling activity of crude extracts of the brown alga *Bifurcaria bifurcata* (Cystoseiraceae) against cyprids of *Balanus amphitrite* and the marine bacteria *Cobetia marina* and *Pseudoalteromonas haloplanktis*. *J. Exp. Mar. Biol. Ecol.* **2004**, *313*, 47−62.

(32) Bakkali, F.; Averbeck, S.; Averbeck, D.; Idaomar, M. Bioligical effects of essentials oils: A review. *Food. Chem. Toxicol.* **2008**, *46*, 446−475.

(33) Fusetani, N. Biofouling and antifouling. *Nat. Prod. Rep.* **2004**, *21*, 94−104.

(34) Timofeeva, L.; Kleshcheva, N. Antimicrobial polymers: Mechanism of action, factors of activity, and applications. *Appl. Microbiol. Biotechnol.* **2011**, *89*, 475−492.
(35) Banerjee, I.; Pangule, R. C.; Kane, R. S. Antifouling coatings: Recent developments in the design of surfaces that prevent fouling by proteins, bacteria, and marine organisms. *Adv. Mater.* **2011**, *23*, 690−718.
(36) Tashiro, T. Antibacterial and bacterium adsorbing macromolecules. *Macromol. Mater. Eng.* **2001**, *286*, 63−87.
(37) Marcotte, L.; Barbeau, J.; Lafleur, M. Permeability and thermodynamics study of quaternary ammonium surfactants-phosphocholine vesicle system. *J. Colloid Interface Sci.* **2005**, *292*, 219−227.
(38) Bressy, C.; Hellio, C.; Marechal, J. P.; Tanguya, B.; Margaillan, A. Bioassays and field immersion tests: a comparison of the antifouling activity of copper-free poly(methacrylic)-based coatings containing tertiary amines and ammonium salt groups. *Biofouling* **2010**, *26*, 769−777.
(39) Chambers, L. D.; Hellio, C.; Stokes, K. R.; Dennington, S. P.; Goodes, L. R.; Wood, R. J. K.; Walsh, F. C. Investigation of *Chondrus crispus* as a potential source of new antifouling agents. *Int. Biodeterior. Biodegrad.* **2011**, *65*, 939−946.
(40) Perkins, R. G.; Mouget, J. L.; Lefebvre, S.; Lavaud, J. Light response curve methodology and possible implications in the application of chlorophyll fluorescence to benthic diatoms. *Mar. Biol.* **2006**, *149*, 703−712.
(41) Dijkman, N. A.; Kromkamp, J. C. Photosynthetic characteristics of the phytoplankton in the Scheldt estuary: community and single-cell fluorescence measurements. *Eur. J. Phycol.* **2006**, *41*, 425−434.
(42) Beer, S.; Vilenkin, B.; Weil, A.; Veste, M.; Susel, L.; Eshel, A. Measuring photosynthesis in seagrasses by pulse amplitude modulated (PAM) fluorometry. *Mar. Ecol.: Prog. Ser.* **1998**, *174*, 293−300.
(43) Eilers, P. H. C.; Peeters, J. C. H. A model for the relationship between light intensity and the rate of photosynthesis in phytoplankton. *Ecol. Model.* **1988**, *42*, 199−215.
(44) Press, W. H.; Teukolsky, S. A.; Vetterling, W. T.; Flannery, B. P. *Numerical Recipes in Fortran 77: The Art of Scientific Computing*, second ed.; Cambridge University Press: Cambridge, 2003.
(45) Ratkowski, D. A. Non Linear Regression Modeling. *A Unified Practical Approach*; Marcel Dekker. Inc.: New York, 1988, p 276.
(46) Thomas, T. E.; Robinson, M. G. The physiological effects of the leachates from a self-polishing organotin antifouling paint on marine diatoms. *Mar. Environ. Res.* **1986**, *18*, 215−229.
(47) Underwood, G. J. C.; Paterson, D. M. The importance of extracellular carbohydrate production by marine epipelic diatoms. *Adv. Bot. Res.* **2003**, *40*, 184−240.
(48) Spiegel, S.; Bader, K. P. Interaction of quaternary ammonium and phosphonium salts with photosynthetic membranes. *Z. Natuforsch.* **2001**, *56*, 1057−1066.
(49) Cooksey, B.; Cooksey, K. E. Calcium is necessary for motility in the diatom *Amphora coffeaeformis*. *Plant Physiol.* **1980**, *65*, 129−131.
(50) Poulsen, N. C.; Spector, I.; Spurck, T. P.; Schultz, T. F.; Wetherbee, R. Diatom gliding is the result of an actin-myosin motility system. *Cell Motil. Cytoskeleton* **1999**, *44*, 23−33.
(51) Verret, F.; Wheeler, G.; Taylor, A. R.; Farnham, G.; Brownlee, C. Calcium channels in photosynthetic eukaryotes: implications for evolution of calcium-based signalling. *New Phytol.* **2010**, *187*, 23−43.
(52) McLachlan, D. H.; Underwood, G. J. C.; Taylor, A. R.; Brownlee, C. Calcium release from intracellular stores is necessary for the photophobic response in the benthic diatom *Navicula perminuta* (Bacillariophyceae). *J. Phycol.* **2012**, *48*, 675−681.
(53) Bothwell, J. H. F.; Ng, C.K.-Y. The evolution of Ca^{2+} signalling in photosynthetic eukaryotes. *New Phytol.* **2005**, *166*, 21−38.
(54) Taylor, A. R. A fast Na^{+}/Ca^{2+}-based action potential in a marine diatom. *PLoS ONE* **2009**, *4*, e4966 DOI: 10.1371/journal.-pone.0004966.
(55) Mishra, S. R.; Sabat, S. C. Calcium and magnesium effect on divalent cation deficient *Hydrilla verticillata* thylakoid electron transport activity. *J. Biosci.* **1988**, *23*, 201−207.
(56) Dau, H. Molecular mechanisms and quantitative models of variable photosystem II fluorescence. *Photochem. Photobiol.* **1994**, *60*, 1−23.
(57) Vrettos, J. S.; Stone, D. A.; Brudvig, G. W. Quantifying the ion selectivity of the Ca^{2+} site in photosystem II: Evidence for direct involvement of Ca^{2+} in O_2 formation. *Biochem.* **2001**, *40*, 7937−7945.
(58) Chen, C. Z.; Beck-Tan, N. C.; Dhurjati, P.; van Dyk, T. K.; LaRossa, R. A.; Cooper, S. L. Quaternary ammonium functionalized poly(propylene imine) dendrimers as effective antimicrobials: Structure−activity studies. *Biomacromolecules* **2000**, *1*, 473−480.